School of Environmental Technology International Conference Proceedings

ISBN: 978-978-54580-8-4

Received: 04 October 2024; Accepted: 20 October 2024; Available online: 07 November 2024

Volume 1 proceedings

Evaluating different satellite-derived bathymetry models: A case study of Tagwai Dam

Tanko R., Ibrahim P. Onoja

Department of Surveying and Geoinformatics Federal University of Technology Minna

geocntric2011@gmail.com

Abstract

Bathymetry entire process involves in a typical survey which is somewhat cumbersome as it involves the general assemble of echo sounder, GPS, Boat (vessel and crew etc. data manipulation and processing is also another rigour to overcome owing to the fact that water surface is dynamic as the water level continuously fluctuates in elevation during the survey. The aim of this research is to determine the underwater topography of Tagwai dam using two empirical methods of Satellite Derived Bathymetry (SDB). The data used where Insitu data (measurements) obtained from EchoMap 50s and accessories and Satellite based data (Landsat 8 OLI 2022). Atmospheric, radiometric and sunglint corrections were performed. OLI and TIRS at Sensor Spectral Radiance was also carried out. Land Use Land Cover classification was performed using the maximum likelihood classification algorithm. The Optimal Band Image Analysis (OBIA) and Stumpf models were employed in this research. The Root Mean Square Error analysis was also carried out to validate the results of the two methods. The results of this research show. both models had a close depth estimation, but the OBIA model had a better depth estimation with RMSE of 0.801124974 against 0.802449293. In estimating maximum and minimum depths from both models, where INSITU max is 8.8m, Stumpf had 1.290463 and OBIA had 1.318488m. where INSITU min was 0.9, both models estimated the min value of 1.314712m. On the general note, Stumpf model had maximum and minimum depth estimation of 1.35107 and 1.203045m respectively. On the other had OBIA had maximum and minimum depths of 1.3561 and 1.11067m. OBIA is recommended for this type of exercise since it give ample opportunity to vary the bands combinations. Although the depths obtained did not exactly correspond with the INSITU data obtained from Echo Sounder, but this research has clearly demonstrated the applicability of Satellite remote sensing in the Hydrographic Surveying.

Keywords: Satellite Derived Bathymetry, Atmospheric correction, Optimal Band Image, Stumpf

1. Introduction

The science of Bathymetry is imperative in understanding how global Earth processes interrelate as they impact the flow of the sea water. Thereby taking heat, salt, nutrients, and pollutants. Underwater surveys (Bathymetry) also helps in understanding the transmission of energy from undersea seismic events that influence navigation and commerce, and shape habitats for marine life, particularly in coastal areas (Paterson *et al* 2011 and Robertson 2016). Coastal areas are always affected by constant pressure due to extreme anthropogenic activities such as agriculture, industrialization, urbanisation, mineral exploitation and climate change-induced natural hazards (e.g., coastal erosion due to sea level changes) (Paterson *et al* 2011). In recent times, Geospatial data has witnessed considerable responsiveness on the global scale. This increasing demand includes the marine-base geospatial data. Bathymetry measurements in oceans, rivers, or lakes are essential, especially in coastal areas with intense use of the coastal zone, heavy sea traffic, and vulnerable natural ecosystems. Monitoring of coastal areas is, thus, of great importance to implement sustainable coastal development and ecosystem protection strategies (Klemas, 2009, Benveniste *et al* 2019, Melet 2020). High spatiotemporal resolution and a vertical accuracy topographic and bathymetric data are also essential not only for understanding coastal systems evolution (Benveniste *et al* 2019), but also for other environmental applications, such as benthic habitat mapping (Janowski etal 2021), seabed geomorphology (Summers *et al* 2021), underwater archaeology (Madricardo *et al* 2021), monitoring of coastal morphological changes, navigation, and fishing (Mason 2000). Traditional methods for estimating sea-bottom surface include Single Beam Echo Sound (SBES) and Multi-Beam Echo Sound (MBES) installed on boats (Samaila-Ija *et al* 2014), as well as active sensor systems LIDAR installed on aerial platforms, remotely controlled vehicles (RVs) and autonomous underwater vehicles (AUVs) (Janowski *et al* 2021; Ajayi and Palmer, 2019). Recently, contemporary maritime space applications required more comprehensive bathymetric data (International Hydrographic Organization IHO, 2005). The increasing demand for detailed bathymetric information ultimately has enhanced hydrographic surveying industry to diversify data collection techniques. The need for more

comprehensive and accurate seabed topography outlook has developed the bathymetry acquisition technique from shipborne platform to airborne and even using space-borne acquisition (Pe'eri *et al* 2014). Satellite Derived Bathymetry (SDB) is a technique based on the empirical, semi-analytical or analytical modelling of light transmission through the atmosphere and the water column. SDB offers great advantages to the planning and executing of hydrographic activities (Randazzo *et al* 2020). The entire process involves in a typical survey is somewhat cumbersome as it involves the general assemble of echo sounder, GPS, Boat (vessel and crew etc. data manipulation and processing is also another rigour to overcome owing to the fact that water surface is dynamic as the water level continuously fluctuates in elevation during the survey (Pe'eri *et al* 2014). Therefore, this research seeks to evaluate the accuracy of underwater topography of Tagwai dam using two empirical methods of Satellite Derived Bathymetry (SDB) models with a view to affirm the most accurate SDB in determining underwater topography.

1.1 Study Area

The study area for this research is Tagwai dam reservoir located in Chanchaga Local Government Area, The dam lies on Latitude 9° 33'55" to 9° 36'07N and Longitude 6° 39' 20" to 6° 39'58"E. The dam is at east of Tunga Goro about 10km, south-east of Mobil Market & North-East of Paiko.

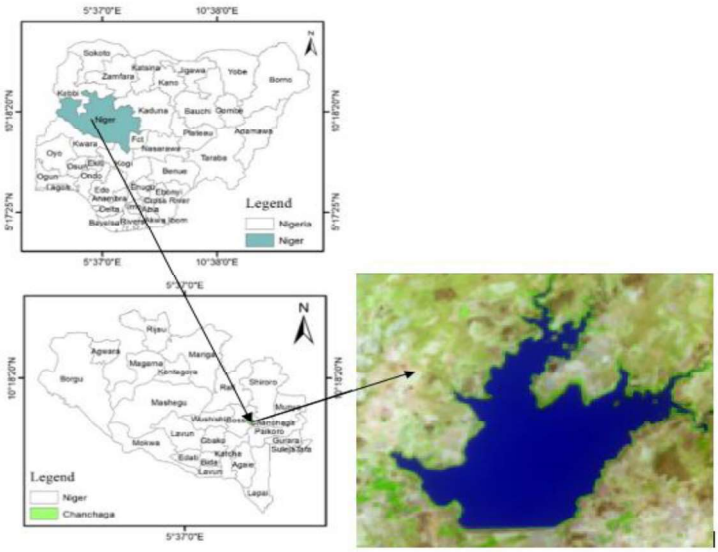

Figure 1. Study area map

2.0 Methodology

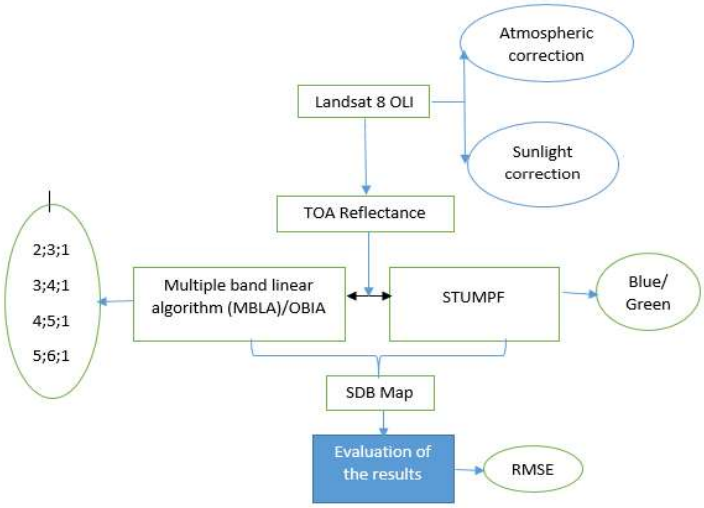

Figure 2. Flowchart of Methodology

2.1 Materials

The hardware used consist of a Garmin Hand held Global positioning system (Etrex HCx series). The software package – ESRI's ArcMap 10 and Microsoft Excel 2010.

2.2 Data Needed

1. Insitu data (measurements): data that obtained from the sounding operation by the use of traditional method. That is the use of EchoMap 50s and accessories.
2. Satellite based data: satellite image that was downloaded from the web. The image is from the Landsat instruments.

Table 1. Landsat Satellite image details

S/N	Satellite	Date	Row/Path	Spatial resolution (m)
1	Landsat 8 OLI	Jan/2022	53/189	30

2.3 Data Processing

2.3.1 Satellite image preproecssing

The atmospheric correction, Radiometric calibration and Sunglint Correction were carried outon the Landsat image downloaded.

2.3.2 OLI and TIRS at Sensor Spectral Radiance

These values are then converted to 16-bit integer values in the finished Level 1 product. These values can then be converted to spectral radiance using the radiance scaling factors provided in the metadata file:

$$L_\lambda = M_L * Q_{cal} + A_L \quad (1)$$

where:

L_λ = Spectral radiance (W/(m2 * sr * μm))

M_L = Radiance multiplicative scaling factor for the band (RADIANCE_MULT_BAND_n from the metadata)

A_L = Radiance additive scaling factor for the band (RADIANCE_ADD_BAND_n from the metadata).

Q_{cal} = L1 pixel value in DN. Extracted Data from MTL file of Landsat 8 OLI image.

M_L = 1.2949E-02. A_L = -64.74290. Q_{cal} = B1

2.3.2 OLI Top of Atmosphere Reflectance

The 16-bit integer values in the L1 product can also be converted to TOA reflectance. The following equation is used to convert Level 1 DN values to TOA reflectance:

$$\rho'_\lambda = M_\rho * Q_{cal} - A_\rho \quad (2)$$

where:

ρ'_λ= TOA Planetary Spectral Reflectance, without correction for solar angle. (Unitless) M_ρ=Reflectance multiplicative scaling factor for the band (REFLECTANCEW_MULT_BAND_n from the metadata). A_ρ= Reflectance additive scaling factor for the band (REFLECTANCE_ADD_BAND_N from the metadata). Q_{cal} = L1 pixel value in DN

Note that ρ_λ' is not true TOA Reflectance, because it does not contain a correction for the solar elevation angle. Once a solar elevation angle is chosen, the conversion to true TOA Reflectance is as follows:

$$\rho_\lambda = \rho'_\lambda \Big/ \sin(\emptyset) \quad (3)$$

where:

ρλ = TOA Planetary Reflectance (Unitless) θ = Solar Elevation Angle (from the metadata, or calculated) M_ρ= 2.0000E-05

A_ρ= -0.100000Q_{cal}= L1 pixel value in DN (Bands) ∅= 49.89416314 (degree) or 0.870375956997777 (radiance)

2.3.3. Optimal Band Ratio Analysis (Obra) Method

The OBRA method of Legleiter *et al.* (2009) uses optimal spectral band pairs for a range of water depths and substrate types. It identifies spectral band pairs that are minimally affected by bottom type variabilities; more specifically, two spectral bands with a high coefficient of determination (R^2). The bathymetric information is subsequently determined by applying Equation below.

$$R_{SDB} = \frac{In(nRw(\lambda i)}{In(nRw(\lambda j)} \quad 4$$

$$Z_{SDB} = m_1 R_{SDB} - m_0 \quad 5$$

where λi is spectral band i, λj is spectral band j, Rw (dimensionless) is observed spectral reflectance and R_{SDB} is the relative satellite-derived bathymetry obtained from a pair of spectral bands.

2.3.4 Stumpf Model

This method argues that the ratio for two zones at a constant depth will be the same, regardless of the difference in the shade of the bottom and can be calculated using actual depths on clear shallow water using only visible bands. The ratio transform algorithm can be apply with bands having different water absorption and can be applied in appropriate wavelengths of any sensor. The values of these zones were applied to the following equation to estimate bathymetry:

$$Z_{SDB} = m_1 \frac{In(n * R(\lambda b)}{In(n * R(\lambda g)} - m_0 \quad 7$$

where Z_{SDB} is the satellite derived bathymetry depth. m_0 is the offset for a depth of 0 m, m_1 is a coefficient to tune the model to the actual depth, R(λb) and R(λg) are the remote sensing radiances for optical bands λ_b (blue band) and λg (green) while n = given as 100. Stumpf's algorithm takes the form of straight-line equation.

$$Y = m_1 X - m_0 \quad 8$$

where m_1 and m_0 is a tuneable constant to scale the ratio to depth, In the ratio model, only two parameters (m_1 and m_0) are need to be estimated. A median filter of 5×5 was used to succeed the reduction of the noise of high frequency.

Twelve points (stations) were selected within the entire 901 sounding points displayed in the study area. These points (Tests) as popularly called in this research are displayed in Figure 4.

2.3.5 Model results Validation

The RMSE was employed in this research as statistical tools for validation in order to compare the accuracy of the extracted results as shown in equations 11 and 12 below.

$$RMSE = \frac{1}{n}\sum_{j=1}^{1} |Z_{SDB} - Z_{FB}| \quad 9$$

where n is the number the field points, Z_{SDB} is the satellite derived bathymetry depth and Z_{FB} is the field point depth.

3. Results and Discussion

A total of 901 sounding points in Tagwai dam were plotted and it can be seen that not all parts of the dam was covered with sounding data which was obtained through the traditional method popularly known as Bathymetry method. From the above displayed data, test points were carefully selected to avoid biasness in the analysis. This is to ensure a good level of spatial distribution of the test points over the surface of the dam. This can be seen in the Figure 3 below.

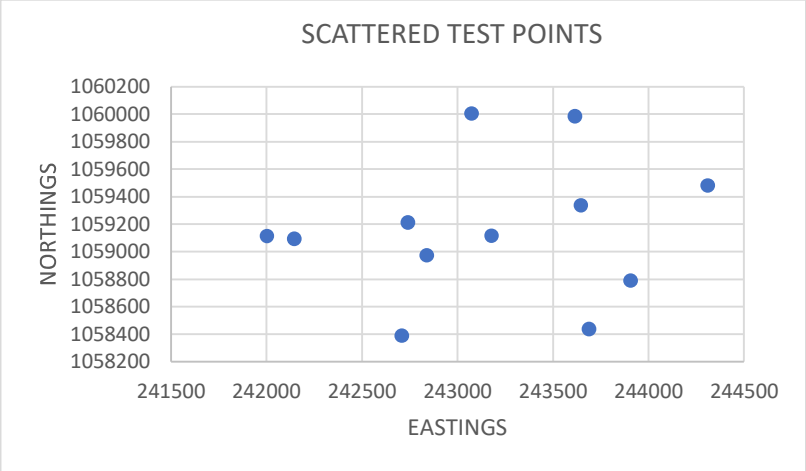

Figure 3. Spatial distribution of Test points

The selection of these points cuts across shallow, medium and high depths as much as possible. this is to balance some claims and assertions when it comes to depths analysis in hydrography.

Table 2: OBIA model

S/No	Easting(m)	Northing(m)	W/ depth	Abs W/ depth (X)	Ratio_Depth (Y1)	Ratio_Depth (Y2)	Ratio_Depth (Y3)
1	242002.1	1059115	-1.1	1.1	1.019454	1.01138	1.11067
8	242146	1059095	-1.6	1.6	1.018667	1.086293	1.18379
137	242708.3	1058389	-8.8	8.8	1.018738	1.076672	1.318499
157	242740	1059213	-1.1	1.1	1.018928	1.113127	1.288689
177	242840	1058974	-5.8	5.8	1.019917	1.120973	1.33426
230	243074	1060006	-1.2	1.2	1.020151	1.114954	1.32889
598	243177.9	1059117	-4.9	4.9	1.020147	1.127098	1.35122
728	243614.6	1059986	-1.1	1.1	1.022758	1.095977	1.311855
741	243646	1059337	-2.9	2.9	1.020102	1.12911	1.3561
759	243688.9	1058438	-1.7	1.7	1.019703	1.049608	1.238
785	243907.4	1058791	-2.2	2.2	1.022946	1.073014	1.267077
801	244310.6	1059482	-0.9	0.9	1.018267	1.114135	1.314712

Table 2 display of satellite derived depths from OBIA model. Y1 has a regression coefficient (r) of 0.1543, Y2 has 0.1584 and Y3 is 0.3794. This was extracted from the twelve test points selected earlier for this research. This was entered side by side with the existing water depth obtained from sounding method serving as ground truth data for this research. The optimal band combination was that of NIR and SWIR which gave the Y^3 ratio depth after linear regression analysis which gave the best regression line as shown below in Figure 4. Other bands combinations were not selected because of a poor linear relationship exhibited

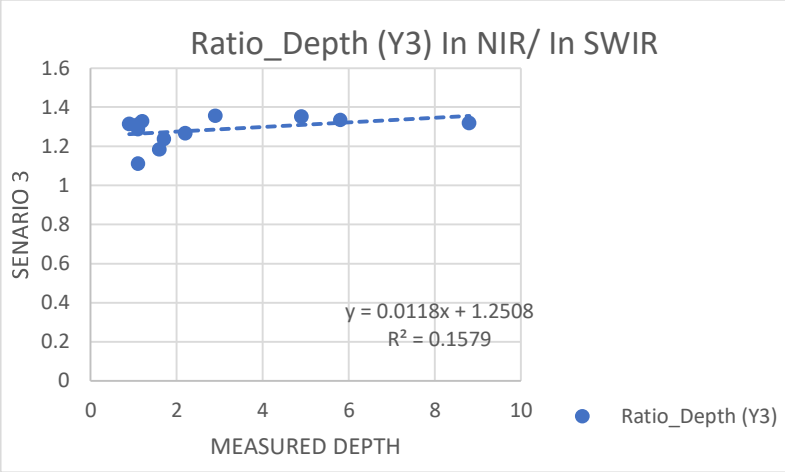

Figure 4. Linear regression of OBIA (Y3) NIR vs SWIR bands

Table 3 STUMPF model (blue/green)

S/No	Easting(m)	Northing(m)	W/ depth	Abs W/ depth (X)	Ratio_Depth (Y)
1	242002.096	1059115.06	-1.1	1.1	1.203045
8	242146	1059095	-1.6	1.6	1.287915
137	242708.338	1058389.074	-8.8	8.8	1.290463
157	242740	1059213	-1.1	1.1	1.318499
177	242840.026	1058974.444	-5.8	5.8	1.33546
230	243074	1060006	-1.2	1.2	1.326728
598	243177.934	1059116.976	-4.9	4.9	1.35127

728	243614.635	1059986.48	-1.1	1.1	1.311855
741	243646.009	1059337.237	-2.9	2.9	1.3561
759	243688.857	1058438.258	-1.7	1.7	1.295309
785	243907.436	1058791.188	-2.2	2.2	1.267077
801	244310.608	1059482.167	-0.9	0.9	1.314712

Table 3 is the Stumpf model displaying the depths obtained at the same tests points earlier selected in this research. The results are also entered side by side with existing ground truth data obtained from the sounding operation.

3.1 Validation Of Results From Two Models

Table 4 Models validation with INSITU data

S/No	Abs W/ depth (X)	OBIA(1)	STUMP(2)	del 1	del2	Sqdel1	Sqdel2
1	1.1	1.11067	1.203045	-0.01067	-0.103045	0.000113849	0.010618272
8	1.6	1.18379	1.287915	0.41621	0.312085	0.173230764	0.097397047
137	8.8	1.318499	1.290463	7.481501	7.509537	55.97285721	56.39314595
157	1.1	1.288689	1.318499	-0.188689	-0.218499	0.035603539	0.047741813
177	5.8	1.33426	1.33546	4.46574	4.46454	19.94283375	19.93211741
230	1.2	1.32889	1.326728	-0.12889	-0.126728	0.016612632	0.016059986
598	4.9	1.35122	1.35127	3.54878	3.54873	12.59383949	12.59348461
728	1.1	1.311855	1.311855	-0.211855	-0.211855	0.044882541	0.044882541
741	2.9	1.3561	1.3561	1.5439	1.5439	2.38362721	2.38362721
759	1.7	1.238	1.295309	0.462	0.404691	0.213444	0.163774805
785	2.2	1.267077	1.267077	0.932923	0.932923	0.870345324	0.870345324
801	0.9	1.314712	1.314712	-0.414712	-0.414712	0.171986043	0.171986043
					SUM	92.41937635	92.72518102
					RMSE	0.801124974	0.802449293

Table 5: Summary of RMSE

S/N	METHOD	RMSE
1	OBIA	0.801124974
2	STUMP	0.802449293

Tables 4 and 5 are the showing the processes involve in the validation of the two models results obtained in this research work. The differences were first determined, and absolute values obtained. The RMSE was determined and OBIA method performed belter that Stumpf method with error analysis of 0.801124974 against 0.802449293. This shows that both models tried to estimate the depths at a very close level of competition with very little difference at each other.

3.2 Models Performance Analysis Base on Various Depth Ranges

Table 6 SHALLOW Depth Range (m) 0.0-1.9

STN	W/depth	Z/depth (OBIA)	Z/depth (STUMP)	del 1	del 2	del 1^2	del 2^2
801	0.9	1.314712	1.314712	-0.414712	-0.414712	0.171986043	0.171986043
759	1.7	1.238	1.295309	0.462	0.404691	0.213444	0.163774805

728	1.1	1.311855	1.311855	-0.211855	-0.211855	0.044882541	0.044882541
230	1.2	1.32889	1.326728	-0.12889	-0.126728	0.016612632	0.016059986
157	1.1	1.288689	1.318499	-0.188689	-0.218499	0.035603539	0.047741813
8	1.6	1.18379	1.287915	0.41621	0.312085	0.173230764	0.097397047
1	1.1	1.11067	1.203045	-0.01067	-0.103045	0.000113849	0.010618272
					SUM	0.655873368	0.552460508
					RMSE	**0.115694299**	**0.10618241**

Table 7 MODERATE Depth Range (m) 2.0-2.29

STN	W/depth	Z/depth (OBIA)	Z/depth (STUMP)	del 1	del 2	del 1^2	del 2^2
785	2.2	1.267077	1.267077	0.932923	0.932923	0.870345324	0.870345324
741	2.9	1.3561	1.3561	1.5439	1.5439	2.38362721	2.38362721
					SUM	3.253972534	3.253972534
					RMSE	**0.901938542**	**0.901938542**

Table 8 HIGH Depth Range (m) 4.0-8.9

STN	W/depth	Z/depth (OBIA)	Z/depth (STUMP)	del 1	del 2	del 1^2	del 2^2
598	4.9	1.35122	1.35127	3.54878	3.54873	12.59384	12.59348
177	5.8	1.33426	1.33546	4.46574	4.46454	19.94283	19.93212
137	8.8	1.318499	1.290463	7.481501	7.509537	55.97286	56.39315
					SUM	88.50953	88.91875
					RMSE	**3.135983**	**3.143225**

SHALLOW Depth Range (m) 0.0-1.9 estimation as seen in Table 6, the Stumpf model performed better that OBIA model with a RMSE of 0.10618241 against 0.115694922 for OBIA. In the MODERATE Depth Range (m) 2.0-2.29 analysis as shown in Table 7, both models had the same RMSE of 0.901938542 and finally the HIGH Depth Range (m) 4.0-8.9, OBIA had a better RMSE of 3.135983 against the Stumpf model of 3.143225 as shown in Table 8 .

4.0 Conclusion

The analysis of the two models shows that both models closely estimated the INSITU data which serve as control information of the underwater topography. The study shows that the OBIA is a better model to adopt when it is about depth estimation using satellite remote sensing method. The estimated error analysis using the RMSE shows that 0.801124974 against 0.802449293 was obtained in this study. In estimating maximum and minimum depths from both models, where INSITU max is 8.8m, Stumpf had 1.290463 and OBIA had 1.318488m. where INSITU min was 0.9, both models estimated the min value of 1.314712m. On the general note, Stumpf model had maximum and minimum depth estimation of 1.35107 and 1.203045m respectively. On the other had OBIA had maximum and minimum depths of 1.3561 and 1.11067m Satellite Derived Bathymetry was successfully carried out in the study which depicts the underwater topography using Landsat 8 OLI image of 2022. Although the depths obtained did not exactly correspond with the INSITU data obtained from echo sounder but this research has clearly demonstrated the applicability of Satellite remote sensing in the Hydrographic Surveying.

References

Paterson, D.M.; Hanley, N.D.; Black, K.; Defew, E.C.; Solan, M. (Eds.) 2011 Biodiversity, ecosystems and coastal zone management: Linking science and policy. Theme Section. Mar. Ecol. Prog. Ser. 2011, 434, 201–301. [CrossRef]

Robertson, E. 2016 Crowd-Sourced Bathymetry Data via Electronic Charting Systems. ESRI Ocean GIS Forum, 2016. Available online: http://proceedings.esri.com/library/userconf/oceans16/papers/oceans_12.pdf (accessed on 20 April 2024).

Klemas, V.V. 2009 The Role of Remote Sensing in Predicting and Determining Coastal Storm Impacts. J. Coast. Res. 2009, 256, 1264–1275.

Ajayi, O. G., & Palmer, M. (2020). Modelling 3D Topography by comparing airborne LiDAR data with Unmanned Aerial System (UAS) photogrammetry under multiple imaging conditions. *Journal of Geomatics and Planning.* 6(2), 122-138, https://doi.org/10.14710/geoplanning.6.2.122-138

Benveniste, J.; Cazenave, A.; Vignudelli, S.; Fenoglio-Marc, L.; Shah, R.; Almar, R.; Andersen, O.; Birol, F.; Bonnefond, P.; Bouffard, J.; 2019. Requirements for a Coastal Hazards Observing System. Front. Mar. Sci. 2019, 6, 348.

Melet, A.; Teatini, P.; Le Cozannet, G.; Jamet, C.; Conversi, A.; Benveniste, J.; Almar, R. 2020 Earth Observations for Monitoring Marine Coastal Hazards and Their Drivers. Surv. Geophys. 2020, 41, 1489–1534.

Samaila-Ija, H. A., Ajayi, O. G., Zitta, N., Odumosu, J. O., Kuta, A. A., Adesina, E. A., Ibrahim, P. (2014). Bathymetric survey and volumetric analysis for sustainable management: case study of Suleja Dam, Niger State, Nigeria. *Journal of Environment and Earth Sciences*. 4(18), 24-35.

Stumpf, R. P., Holderied, K. and Sinclair, M., 2003. Determination of Water Depth with HighResolution Satellite Imagery over Variable Bottom Types. Limnology Oceanography, 48, 547-556

Janowski, L.; Wroblewski, R.; Dworniczak, J.; Kolakowski, M.; Rogowska, K.; Wojcik, M.; Gajewski, J. 2021 Offshore benthic habitat mapping based on object-based image analysis and geomorphometric approach. A case study from the Slupsk Bank, Southern Baltic Sea. Sci. Total Environ. 2021, 801, 149712.

Summers, G.; Lim, A.; Wheeler, A. A Scalable, 2021 Supervised Classification of Seabed Sediment Waves Using an Object-Based Image Analysis Approach. Remote Sens. 2021, 13, 2317

Madricardo, F.; Bassani, M.; D'Acunto, G.; Calandriello, A.; Foglini, F. 2021. New evidence of a Roman road in the Venice Lagoon (Italy) based on high resolution seafloor reconstruction. Sci. Rep. 2021, 11, 13985

Mason, D.C.; Gurney, C.; Kennett, M. 2000. Beach topography mapping—A comparison of techniques. J. Coast. Conserv. 2000, 6, 113–124

International Hydrographic Organization, 2005. Manual on Hydrography (1st Edition: Corrections to February 2011). Monaco: IHO Publication C-13.

Pe'eri, S., Parrish, C., Azuike, C., Alexander, L. and Armstrong, A., 2014. Satellite Remote Sensing as Reconnaissance Tool for Assessing Nautical Chart Adequacy and Completeness. Marine Geodesy, 37, 293–314.

Randazzo, G.; Barreca, G.; Cascio, M.; Crupi, A.; Fontana, M.; Gregorio, F.; Lanza, S.; Muzirafuti, A. Analysis of Very High Spatial Resolution Images for Automatic Shoreline Extraction and Satellite-Derived Bathymetry Mapping. Geoscience 2020, 10, 172.